SIRT6 promotes ferroptosis and attenuates glycolysis in pancreatic cancer through regulation of the NF-κB pathway

SHUANGXI GONG[1], LIXIN XIONG[2], ZHEN LUO[1], QINGHUA YIN[2], MING HUANG[2], YANG ZHOU[2] and JIAN LI[2]

Departments of [1]General Surgery and [2]Hepatobiliary Surgery,
The First Hospital of Changsha, Changsha, Hunan 410005, P.R. China

Received November 26, 2021; Accepted March 16, 2022

DOI: 10.3892/etm.2022.11430

RETRACTED

Abstract. Pancreatic cancer (PC) is a malignant tumor with high mortality worldwide. SIRT6 plays versatile roles in human cancers. However, SIRT6 has rarely been studied in PC. The purpose of the present study was to explore the function and potential mechanism of SIRT6 in PC. The expression of SIRT6 in PC tissues and cells was detected by reverse transcription-quantitative PCR and western blotting. The overall survival time was analyzed through the Kaplan Meier method. Cell viability was measured by the Cell Counting Kit-8 assay. The Fe^{2+} content, glucose uptake, lactic acid and ATP production were detected through the corresponding kits. ROS was evaluated using the DCFH-DA detection kit. Protein expression was assessed by immunohistochemistry or western blot analysis. In the present study, SIRT6 was lowly expressed in PC tissues and cells compared with normal tissues and cells. Moreover, the low expression of SIRT6 was associated with a poor prognosis in patients with PC. Upregulation of SIRT6 significantly promoted the ferroptosis and inhibited the glycolysis in PC cells. However, knockdown of SIRT6 resisted ferroptosis and increased glycolysis in PC cells. Further studies found that the activation of NF-κB could reverse the effect of SIRT6 on PC cells. In addition, overexpression of SIRT6 restrained the growth of xenografted tumors and suppressed the nuclear transcription of NF-κB *in vivo*. Collectively, the present study indicated that SIRT6 promoted ferroptosis and inhibited glycolysis through inactivating the NF-κB signaling pathway in PC. These findings suggested that SIRT6 may become a therapeutic target for PC.

Introduction

Pancreatic cancer (PC) is a highly fatal malignancy (1). Its characteristics include low resection rate, insensitivity to radiotherapy and chemotherapy, recurrence and distant metastasis, which cause the poor prognosis (2-4). PC is mainly divided into two types: adenocarcinoma and pancreatic ductal adenocarcinoma (PDAC) (5). It has been reported that PDAC is the most common type of PC, accounting for 85% of all PC cases (6). In addition, K-ras gene mutations exist in 90% of PDAC cases (7). These mutations not only promote malignant proliferation of tumor cells, but also change cell metabolism (7). The molecular mechanisms underlying PC remain unclear and efficacious therapies to overcome this neoplasm are unavailable. Thus, novel therapies for inhibiting PC are urgently needed.

Ferroptosis is a novel form of programmed cell death. Due to the continuous accumulation of iron ions in cells and increase of lipid reactive oxygen species (ROS), cell redox metabolism is destroyed, which finally leads to cell death (8,9). At present, ferroptosis has been found in various types of tumor cells, such as PC, renal cell carcinoma and hepatocellular carcinoma (10-12). The mutation of K-ras gene has been revealed to cause the increase of ROS in PC (13). PC cells alleviate the toxic effect from ROS by synthesizing a large amount of glutathione with antioxidant effect (14). Studies have shown that inhibition of glutathione peroxidase 4 (GPX4) and cystine/glutamate reverse transport system (system XC) could promote the accumulation of ROS and induce ferroptosis in PC cells (15-17). Although the induction of ferroptosis is a promising therapeutic strategy to inhibit cancer cell growth (18), the factors that modulate sensitivity of ferroptosis remain largely vague.

The abnormal glycolysis of tumor cells is called aerobic glycolysis, which is regulated by a variety of tumor specific metabolic enzymes (19). Hexokinase (HK) is the first rate-limiting enzyme of the pathway of glycolysis, and HK2, as one of the four subtypes of HK, was found to be abnormally highly expressed in a variety of tumor cells (20,21). In addition, ferroptosis is often accompanied by inhibition of glycolysis (22). Therefore, investigating thoroughly the molecules or genes that target ferroptosis and glycolysis may be a new direction for the treatment of PC.

Class 3 histone deacetylases (Class 3 HDACs), commonly known as sirtuins (SIRTs), are a class of highly conserved proteins (23). These proteins possess nicotinamide adenine dinucleotide dependent deacetylases and single ADP-ribosyl transferase activities (23). Those demonstrated that SIRTs

Correspondence to: Dr Jian Li, Department of Hepatobiliary Surgery, The First Hospital of Changsha, 311 Yingpan Road, Kaifu, Changsha, Hunan 410005, P.R. China
E-mail: lijianljdoc@126.com

Key words: sirtuin 6, ferroptosis, glycolysis, pancreatic cancer

could participate in regulating ferroptosis and glycolysis. For example, SIRT3 inhibits AKT-dependent mitochondrial metabolism and epithelial-mesenchymal transition (EMT), leading to ferroptosis and tumor suppression (24). HDAC SIRT1 gene silencing or pharmacological inhibition by EX-527 suppressed EMT and consequently decreased ferroptosis, whereas SIRT inducers, resveratrol and SRT1720, increased ferroptosis in head and neck cancer cells (25). SIRT6 gene is located on chromosome 19 (19p13.3), and the encoded protein belongs to the homologous protein family of Sir2 (26). SIRT6 is located in the nucleus and participates in a variety of biological processes, including aging, chromatin regulation, transcriptional regulation, glucose metabolism, fat metabolism and DNA damage repair (27,28). Moreover, SIRT6 plays an important role in the development of cancer (29). SIRT6 knockout could inhibit the transcriptional activities of MYC and HIF1α, increase glycolysis and promote abnormal tumor proliferation (30). In hepatocellular carcinoma, overexpression of SIRT6 activated the extracellular signal regulated kinase 1/2 pathway, promoted apoptosis and reduced ROS (31). However, the function of SIRT6 in PC has been rarely studied.

In the present study, it was explored whether SIRT6 could affect PC progression by regulating ferroptosis and glycolysis. The present results indicated that SIRT6 increased the level of ROS, promoted ferroptosis and restrained glycolysis *in vitro* and *in vivo* by inhibiting the activation of the NF-κB pathway. The data provided the evidence that SIRT6 could be an anti-PC gene.

Materials and methods

Tissue samples. The tumor tissues and corresponding paracancerous tissues of 68 patients with PC treated between March 2016 and March 2017 in The First Hospital of Changsha (Changsha, China) were collected. All patients did not receive radiotherapy and chemotherapy before operation. Written informed consent was provided by all participants. The present study was approved [(2016) Ethical Review (Clinical Research) approval no. 59] by the Ethics Committee of The First Hospital of Changsha (Changsha, China).

Cell culture. SW1990 (cat. no. CRL-2172), BXPC-3 (cat. no. CRL-1687) and PANC-1 (cat. no. CRL-1469) cells were purchased from the American Type Culture Collection. PC-2 (cat. no. JK-CS1579) and human normal pancreatic epithelial (HPDE; cat. no. JK-CS2033) cells were obtained from Shanghai Jingkang Bioengineering Co., Ltd. The cells were cultured in a constant temperature incubator with 5% CO_2 at 37˚C. The medium used was DMEM containing 10% fetal bovine serum (both from Gibco; Thermo Fisher Scientific, Inc.).

Cell transfection. PcDNA-SIRT6, vector, small interfering (si)-SIRT6#1 (5'-CCA AGUGUA AGACGC AGUATT-3'), si-SIRT6#2 (5'-TCATGACCCGGCTCATGAA-3'), si-SIRT6#3 (5'-CGAGGAUGUCGGUGA AUUA-3') and si-NC (5'-GGC CAAGCCUUGUGUAA AU-3') were obtained from Shanghai GenePharma Co., Ltd. PANC-1 or SW1990 cells were inoculated into six-well plates and cultured overnight. According to the manufacturer's protocol of Lipofectamine™ 2000 transfection reagent (Invitrogen; Thermo Fisher Scientific, Inc.), the cells were mixed with the corresponding plasmids, incubated for 6 h in an incubator with 5% CO_2 at 37˚C, and then cultured with fresh medium for 24 h. The concentration of siRNAs was 100 nM and the mass of vector was 2 μg. After 48 h, the overexpression of SIRT6 in PANC-1 cells and downregulation of SIRT6 in SW1990 cells were verified by reverse transcription-quantitative polymerase chain reaction (RT-qPCR) and western blot analysis.

Cell counting Kit-8 (CCK-8) assay. The transfected PANC-1 cells were inoculated into 96-well plates at a concentration of 3,000 cells/well. After 48 h of culture, 10 μl of CCK-8 solution (Beyotime Institute of Biotechnology) was added to each well and the cells were incubated for 2 h at an atmosphere containing 5% CO_2 at 37˚C. The absorbance value at the wavelength of 450 nm was detected using a microplate reader (BioTek Instruments, Inc.).

RT-qPCR. Total RNA of tissues and cells (PANC-1 and SW1990) was isolated using TRIzol® reagent (Invitrogen; Thermo Fisher Scientific, Inc.), and then single stranded cDNA was obtained according to the instructions of Prime ScriptTM RTMaster Mix (Takara Biotechnology Co., Ltd.). Subsequently, the RT-qPCR experiment was carried out according to the protocol of SYBR Premix Ex TaqTM II kit (Takara Biotechnology Co., Ltd.). The expression levels of mRNA were quantified using the $2^{-\Delta\Delta Cq}$ method (32). GAPDH was used as an internal reference gene. The thermocycling conditions for qPCR were as follows: 95˚C for 5 min, and then 40 cycles (95˚C for 10 sec, 60˚C for 30 sec). The following primer pairs were used for qPCR: SIRT6 forward 5'-CAAGTG TAAGACGCAGTACG-3' and reverse, 5'-GATGGTGTCCCT CAGCTCTC-3'; and GAPDH forward, 5'-TGACTTCAACAG CGACACCCA-3' and reverse, 5'-CACCCTGTTGCTGTA GCCAAA-3'.

ROS detection. The PANC-1 and SW1990 cells were inoculated into six-well plates at a density of $2x10^5$/well and cultured for 24 h at 37˚C and 5% CO_2. DCFH-DA (50 μM) (Beyotime Institute of Biotechnology) was added to each well and cells were cultured for 30 min at 37˚C and 5% CO_2. Subsequently, the supernatant was discarded and the cells were washed with PBS for 3 times. Finally, the fluorescence intensity was measured under a fluorescence microscope (Nikon eclipse 80i; Nikon Corporation). The excitation and emission wavelengths were 488 and 525 nm, respectively.

Fe^{2+} content detection. The Fe^{2+} level in PANC-1 and SW1990 cells was detected by Fe^{2+} colorimetry detection kit (catalog no. E1042-100; Applygen Technologies, Inc.). The cells were lysed using RIPA reagent, and the supernatant was collected by centrifugation (10,000 x g, 4˚C, 10 min). Reagent A was obtained by mixing the buffer in the kit and 4.5% potassium permanganate solution at 1:1 ratio. Then, the supernatant was mixed with reagent A at 1:1 ratio according to the manufacturer's instructions and was incubated at 60˚C for 1 h. After cooling at room temperature, Fe^{2+} content was detected using Fe^{2+} detection agent (30 μl, 30 min) in the kit. The absorbance value at 550 nm wavelength was detected using a microplate reader (BioTek Instruments, Inc.).

RETRACTED

Erastin (catalog no. E7781) and ferrostatin-1 (catalog no. S7243) were obtained from Selleck Chemicals. The PANC-1 cells transfected with pcDNA-SIRT6 and the SW1990 cells transfected with si-SIRT6 were treated with erastin (10 μM) or ferrostatin-1 (1 μM) for 24 h, and then the Fe^{2+} level was evaluated.

Western blot analysis. Total protein of tissues or cells (PANC-1 and SW1990) was extracted using RIPA lysis buffer (Beyotime Institute of Biotechnology). Protein content was detected using BCA detection kit (Beyotime Institute of Biotechnology). A total of 30 μg protein sample/well was separated using 10% SDS-PAGE and then transferred to PVDF membranes (MilliporeSigma). Following that, the membranes were incubated for 1 h with 5% skimmed milk powder at room temperature. The membranes were incubated overnight at 4˚C with the corresponding primary antibodies: SIRT6 (1:1,000; catalog no. ab119007), NF-κB p65 (1:1,000; catalog no. ab32536), lamin B (1:1,000; catalog no. ab232731), IκBα (1:1,000; catalog no. ab76429), GPX4 (1:1,000; catalog no. ab125066), SLC7A11 (1:1,000; catalog no. ab37185), HK2 (1:1,000; catalog no. ab104836) and lactate dehydrogenase A (LDHA; 1:1,000; catalog no. ab134187) (all from Abcam). Following the primary incubation, membranes were washed three times with PBST (0.1% Tween20) and then incubated at room temperature for 2 h with the DyLight® 488-conjugated secondary antibodies: Goat anti-rabbit IgG H&L (1:5,000; product code ab96899) or goat anti-mouse IgG H&L (1:5,000; product code ab96879; both from Abcam). Protein bands were visualized using Immobilon ECL Ultra Western HRP (MilliporeSigma). The results were analyzed using ImageJ version 6.0 (National Institutes of Health).

Immunofluorescence. PANC-1 cells ($1x10^5$/ml) transfected with vector or pcDNA-SIRT6 were seeded on a coverslip pre-coated with poly-L-lysine, and cultured in DMEM with or without RANKL (50 ng/ml; Invitrogen; Thermo Fisher Scientific, Inc.). After 24 h of culture, the cells fixed with 4% cold formaldehyde at 4˚C overnight. After washing three times with PBS containing 0.1% Triton X-100, the cells were blocked with 10% bovine serum albumin (MilliporeSigma) for 2 h at room temperature, and then incubated with primary antibodies against NF-κB p65 (1:1,000; catalog no. ab288751) and DAPI (1:2,000; catalog no. ab104139) (both from Abcam) at 4˚C overnight. Cells were then incubated with Alexa Fluor 488 donkey anti-mouse immunoglobulin G (1:200; catalog no. ab150105; Abcam) secondary antibodies for 1 h at room temperature and visualized using a confocal laser-scanning microscope.

Detection of glucose, lactic acid and ATP content. The content of glucose (catalog no. A154-1-1), lactic acid (catalog no. A019-1-1) and ATP (catalog no. A095-1-1) in energy metabolism were detected by corresponding kits (Nanjing Jiancheng Bioengineering Institute). PANC-1 cells in logarithmic growth stage were digested with trypsin, and the cell concentration was adjusted to $2x10^5$/ml with serum-free DMEM medium; cells were then inoculated on 12-well plates and kept at 1 ml per well. After 48 h of culture, the supernatant of cell culture medium was collected, and the glucose and lactic acid levels in the supernatant were determined using the glucose and lactic acid detection kits according to the manufacturer's protocol. In addition, PANC-1 cells were collected and homogenized in a hot water bath (90-100˚C), and then kept for 10 min in a boiling water bath. Following that, the protein concentration and ATP level were determined. In order to avoid the difference in the number of cells between the experimental groups, the content of glucose, lactic acid and ATP were examined for sample standardization by dividing the protein concentration of each sample. Glucose consumption equals to the glucose content of culture medium minus the glucose content of cell culture medium.

Tumorigenesis experiment. Animals were fed under specific-pathogen-free conditions, in the mouse-feeding facility with a 12-h light/dark cycle at 22±2˚C and 50-60% humidity, with free foraging and activity and free access to food and water. A total of 20 SPF BALB/C nude mice were randomly divided into two groups [SIRT6 group (n=10) and vector group (n=10)]. PANC-1 cells ($1x10^6$) in 200 μl phosphate-buffered saline were subcutaneously inoculated in nude mice of each group. The tumor volume was recorded every 7 days. After 4 weeks, the nude mice were euthanized by intraperitoneal injection of 120 mg/kg pentobarbital sodium, and the tumor was stripped and weighed. During the experiment, when dyspnea, diarrhea, incontinence, rapid weight loss, or loss of appetite (more than 24 h without eating and drinking) were observed, the mice should be euthanized. The death of mice was determined by observing the cardiac arrest and pupil dilation. Animal health and behaviour were monitored every 3 days. The animal study was approved [(2016) Ethical Review (Clinical Research) approval no. 59] by the Institutional Animal Care and Use Committee of The First Hospital of Changsha (Changsha, China).

Immunohistochemistry. The tumor tissue was cut into 4.5-μm-thick sections after dehydration, transparency and paraffin embedding. The sections were dewaxed at 60˚C for 20 min with xylene and hydrated for 5 min with absolute, 95 and 80% ethanol solutions, respectively. The slices were soaked for 20 min using 3% hydrogen peroxide, and then placed in a citrate buffer at 95˚C and cooled to room temperature. The sections were blocked for 45 min with 5% bovine serum albumin (MilliporeSigma) at 37˚C. Subsequently, tissue sections were incubated overnight at 4˚C with the following primary antibodies: Ki67 (1:200; product code ab15580), SIRT6 (1:200; product code ab236024), GPX4 (1:100; product code ab125066), SLC7A11 (1:200; product code ab37185), HK2 (1:200; product code ab104836) and LDHA (1:100; product code ab134187; all from Abcam). Following the primary incubation, the sections were incubated for 30 min at 37˚C with the following secondary antibodies: goat anti-rabbit IgG H&L (1:250) or goat anti-mouse IgG H&L (1:250). After DAB staining for 3-5 min at room temperature, the nuclei were counterstained with hematoxylin for 3 min at room temperature. The sections were differentiated with 1% hydrochloric-alcohol, returned to blue with 1% ammonia, dehydrated and made transparent, dried in the air and sealed with neutral resin. Images were captured under a light Olympus BX-41 microscope (Olympus Corporation).

RETRACTED

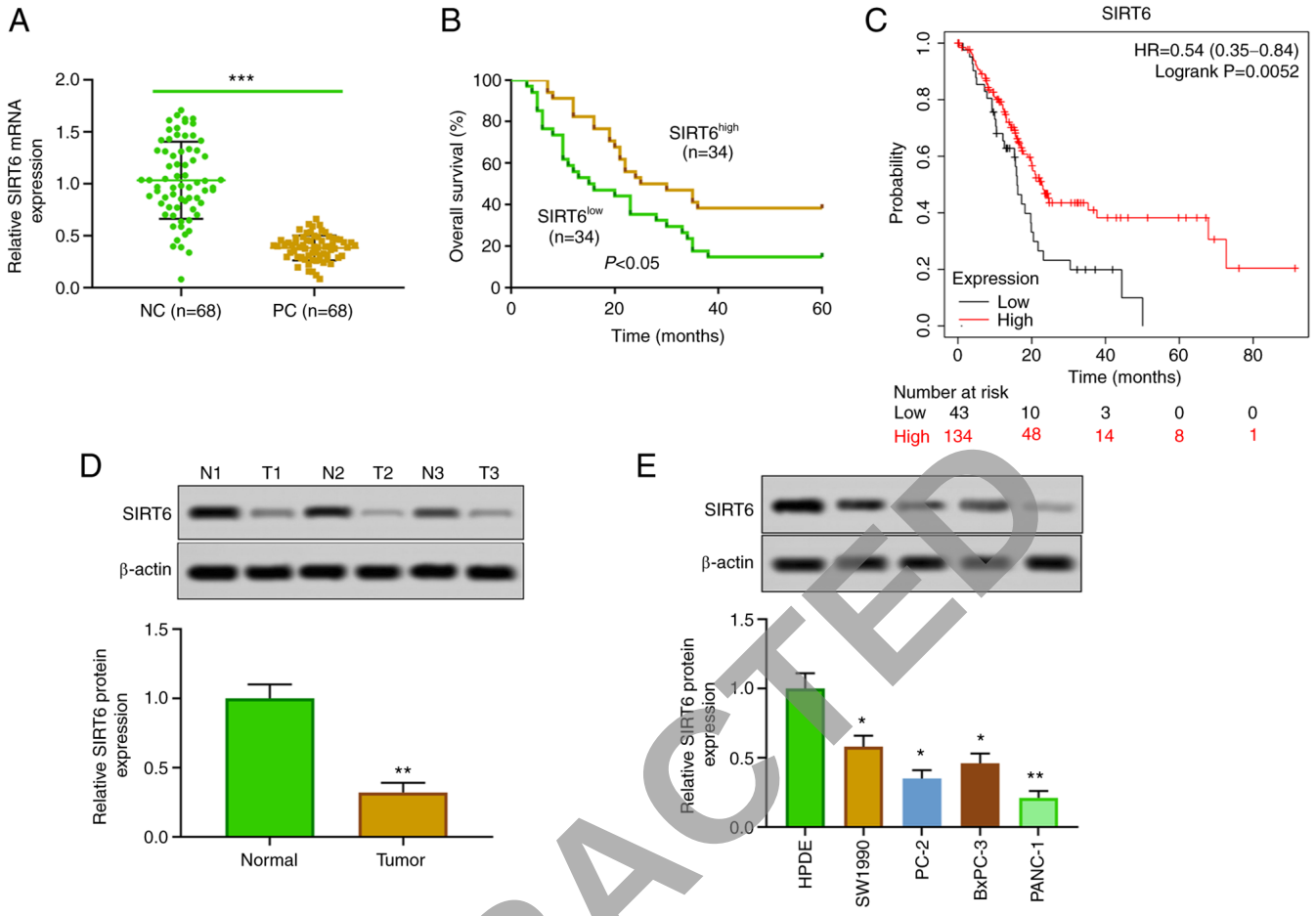

Figure 1. SIRT6 is lowly expressed in pancreatic cancer tissues and cells. (A) The expression of SIRT6 was detected in 68 pairs of PC and paracancerous tissues using reverse transcription-quantitative PCR. (B) Kaplan-Meier survival curve was used to evaluate the overall survival time of patients with PC who had low expression of SIRT6 (n=34) and high expression of SIRT6 (n=34). (C) The survival rate was determined by Kaplan-Meier-plotter online analysis. (D) The expression of SIRT6 in 3 random pairs of PC and adjacent tissues was determined by western blot analysis. (E) Expression of SIRT6 protein in HPDE cells and PC cell lines (SW1990, PC-2, BxPC-3 and PANC-1) was detected by western blotting. ***P<0.001 vs. NC group, **P<0.01 vs. normal and HPDE cells and *P<0.05 vs. HPDE cells. SIRT6, sirtuin6; PC, pancreatic cancer; HPDE, human normal pancreatic epithelial; NC, negative control.

RETRACTED

Statistical analysis. SPSS 30.0 software (IBM Corp.) was used to analyze the data, and the data was expressed as the means ± SD. Paired Student's t-test was used for the comparison between the tumor and corresponding paracancerous tissues, and the remaining two group comparisons were analyzed by unpaired Student's t-test. One-way ANOVA followed by Bonferroni test was used for the comparison among multiple groups. The χ^2 test was used to analyze the relationship between SIRT6 expression and clinicopathological characteristics. Kaplan-Meier analysis followed by the log-rank test (https://kmplot.com/analysis/) was used to estimate the overall survival of PC patients. P<0.05 was considered to indicate a statistically significant difference.

Results

Low expression of SIRT6 in PC. The expression of SIRT6 in PC tissues and cells was detected. The results of RT-qPCR and western blotting revealed that the expression of SIRT6 in PC tissues was lower than that in corresponding adjacent tissues (Fig. 1A and D). Moreover, SIRT6 was significantly downregulated in PC cell lines (SW1990, PC-2, BxPC-3 and PANC-1) compared with HPDE cells (Fig. 1E). In the present experiments, in order to study the effect of upregulation and downregulation of SIRT6 on PC cells, SIRT6 was overexpressed in the low-expressing line (PANC-1 cells), and SIRT6 was silenced in the high-expressing line (SW1990 cells). In addition, our clinical and database data indicated that patients with PC with low expression of SIRT6 had a lower survival rate than the patients with high expression of SIRT6 (Fig. 1B). Furthermore, Kaplan-Meier survival curve analysis showed that patients with PC with low expression of SIRT6 had poor survival, whereas high expression of SIRT6 was positively associated with overall survival (HR=0.54, 95% CI: 0.35-0.84, P=0.0052, Fig. 1C). In addition, our clinical data indicated that the expression of SIRT6 was negatively associated with the distant metastasis, histological grade and TNM stages in patients with PC (Table I). These results suggested that the expression of SIRT6 may affect the progression of PC.

Upregulation of SIRT6 promotes ferroptosis and inhibits glycolysis in PC cells. In order to explore the function of SIRT6 in PC cells, SIRT6 was upregulated by transfection of pcDNA-SIRT6 into PANC-1 cells. The results of RT-qPCR and western blot analysis verified that SIRT6 was overexpressed in PANC-1 cells transfected with pcDNA-SIRT6

Table I. Association between SIRT6 expression and the clinicopathological features of 68 patients with pancreatic cancer.

Clinicopathological characteristics	All cases	Expression level of SIRT6		P-value
		High (n=34)	Low (n=34)	
Sex				0.467
Male	35	19	16	
Female	33	15	18	
Age, years				0.806
<60	29	14	15	
≥60	39	20	19	
Tumor size, cm				0.086
<2	29	18	11	
≥2	39	16	23	
Distant metastasis				0.002[a]
Positive	33	10	23	
Negative	35	24	11	
Histological grade				0.029[b]
High/moderate		13	22	
Low		21	12	
TNM stage				0.027[b]
I/II		19	10	
III/IV		15	24	

[a]P<0.01 and [b]P<0.05 vs. high SIRT6 expression group. SIRT6, sirtuin 6.

RETRACTED

(Fig. 2A and B). The results of CCK-8 showed that the overexpression of SIRT6 inhibited the viability of PANC-1 cells at 48 and 72 h (Fig. 2C). The enhancement of SIRT6 could increase the level of Fe^{2+} in PANC-1 cells (Fig. 2D). The addition of erastin (ferroptosis inducer) further increased the level of Fe^{2+}, but the addition of ferrostatin-1 (ferroptosis inhibitor) reversed that effect (Fig. 2E). Moreover, SIRT6 elevation increased the level of ROS (Fig. 2F) and weakened the expression of GPX4 and SLC7A11 in PANC-1 cells (Fig. 2G). In addition, overexpression of SIRT4 inhibited the glycolysis through inhibiting the production of lactic acid and ATP and reducing glucose uptake in PANC-1 cells (Fig. 2H-J). The expression of HK2 and LDHA was also inhibited (Fig. 2K). These results demonstrated that SIRT6 upregulation increased ferroptosis and inhibited glycolysis in PC cells.

Silencing SIRT6 attenuates ferroptosis and enhances glycolysis in PC cells. SIRT6 was downregulated by transfection of si-SIRT6 (#1, #2 and #3) in SW1990 cells, which was used to further verify the role of SIRT6 in PC cells. The silencing of SIRT6 in SW1990 cells transfected with si-SIRT6 was confirmed by RT-qPCR and western blotting (Fig. 3A and B). The relative expression of SIRT6 was the lowest in si-SIRT6#1-transfected SW1990 cells, which was selected for the subsequent experiments. The silencing of SIRT6 enhanced the viability of SW1990 cells at 48 and 72 h (Fig. 3C). The downregulation of SIRT6 suppressed the content of Fe^{2+} (Fig. 3D), which was enhanced by erastin and weakened by ferrostatin-1 (Fig. 3E). Furthermore, SIRT6 knockout reduced ROS levels (Fig. 3F) and increased the expression of GPX4 and SLC7A11 (Fig. 3G). In addition, the inhibition of SIRT6 promoted glucose uptake, production of lactic acid and ATP (Fig. 3H-J), and enhanced the expression of HK2 and LDHA (Fig. 3K). The aforementioned findings showed that downregulation of SIRT6 restrained ferroptosis and promoted glycolysis in PC cells.

SIRT6 promotes ferroptosis and inhibits glycolysis by inhibiting nuclear transfer of NF-κB p65. In order to study the mechanism of SIRT6 affecting PC, the effect of SIRT6 on the transcriptional regulation of NF-κB p65 was explored. The results of western blot analysis showed that overexpression of SIRT6 increased the expression of IκBα in the cytoplasm, whereas it inhibited the expression of p65 in the nucleus (Fig. 4A). In addition, the results of immunofluorescence assay about p65 expression in the nucleus were consistent with those of western blotting (Fig. 4B). Receptor activator of nuclear factor κB ligand (RANKL), as an agonist of NF-κB p65 nuclear transfer, is commonly used in the study of the NF-κB signaling pathway. The results indicated that RANKL reversed the effects of SIRT6 upregulation on the level of IκBa (cytoplasm) and p65 (nucleus) (Fig. 4C). Cell viability experiments revealed that the decrease of the viability of PANC-1 cells induced by SIRT6 was weakened by RANKL (Fig. 4D). In addition, RANKL blocked the upregulation of ROS in PANC-1 cells induced by SIRT6 (Fig. 4E). Overexpression of SIRT6 inhibited the expression of GPX4, SLC7A11, HK2

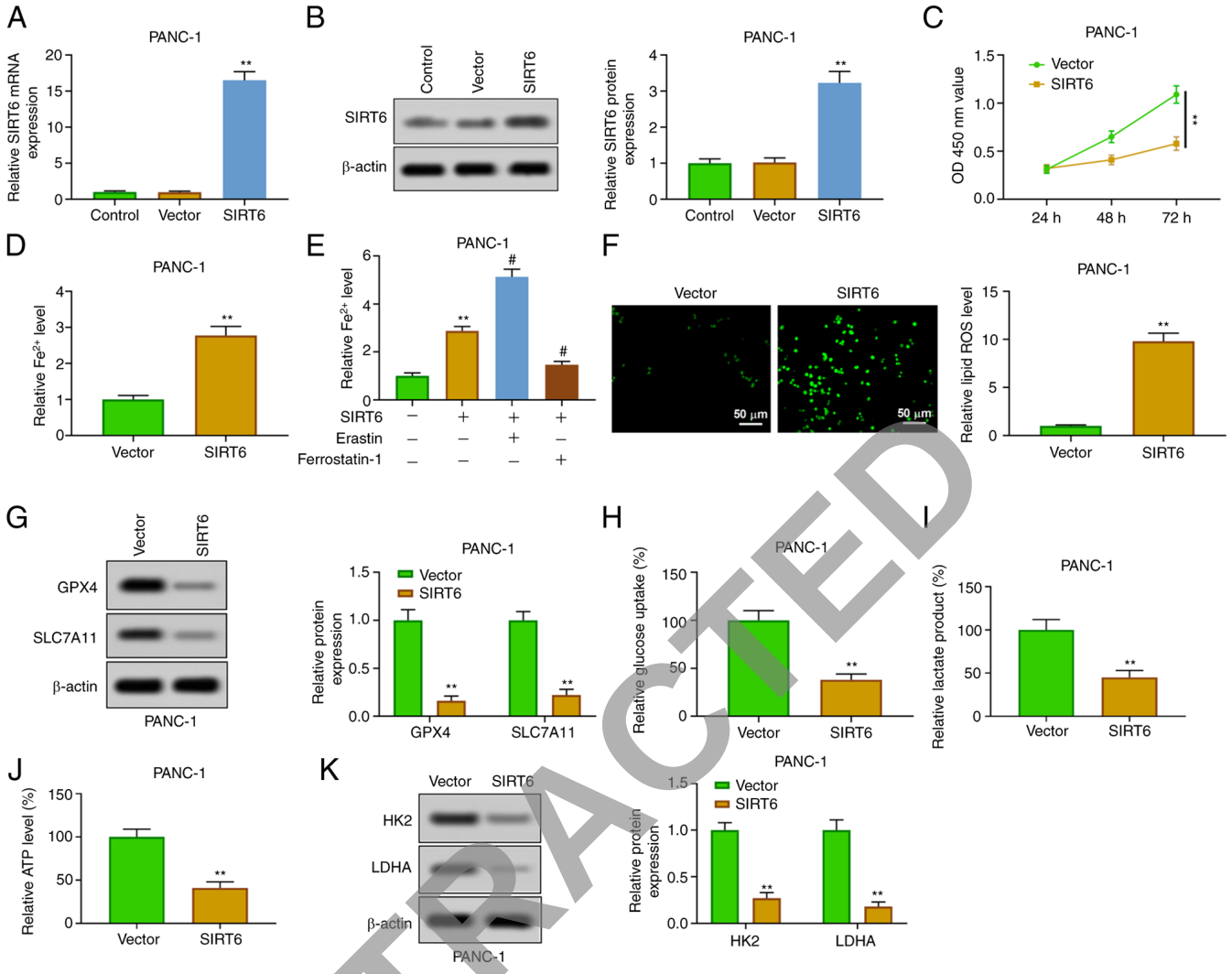

Figure 2. Overexpression of SIRT6 induces ferroptosis and inhibits glycolysis in pancreatic cancer cells. (A and B) After transfection with pcDNA-SIRT6, the expression of SIRT6 in PANC-1 cells was detected by (A) reverse transcription-quantitative PCR and (B) western blotting. (C) The viability of PANC-1 cells was determined by Cell Counting Kit-8 assay. (D) Fe^{2+} content was evaluated by Fe^{2+} detection kit. (E) PANC-1 cells transfected with pcDNA-SIRT6 were treated with erastin or ferrostatin-1, and then Fe^{2+} content was evaluated by Fe^{2+} detection kit. (F) ROS level was detected by DCFH-DA method. (G) GPX4 and SLC7A11 expression levels were assessed by western blot analysis. (H-J) Glucose consumption, lactic acid and ATP production were evaluated by the corresponding kits. (K) HK2 and LDHA expression levels were detected by western blotting. $^{**}P<0.01$ vs. control and vector group and $^{\#}P<0.05$ vs. SIRT6 group. SIRT6, sirtuin6; ROS, reactive oxygen species; GPX4, glutathione peroxidase 4; HK, hexokinase; LDHA, lactate dehydrogenase A.

RETRACTED

and LDHA, whereas RANKL reversed these effects (Fig. 4F). These results indicated that SIRT6 inhibited tumor characteristics of PC by activating the NF-κB signaling pathway.

SIRT6 inhibits the growth of PC xenografts in vivo. To confirm the oncological properties of SIRT6 *in vivo*, a xenografted tumor model was established by injecting PANC-1 cells subcutaneously into nude mice. The results showed that the upregulation of SIRT6 could inhibit the volume of tumor (Fig. 5A) and had no effect on the body weight of mice (Fig. 5B). Concurrently, the weight of the tumor was also reduced by SIRT6 overexpression (Fig. 5C). Immunohistochemical results revealed that SIRT6 was upregulated, and the expression levels of Ki67, GPX4, SLC7A11, HK2 and LDHA were inhibited in the xenografted tumor tissues of mice of the SIRT6-overexpression group (Fig. 5D). Moreover, the upregulation of SIRT6 increased the cytoplasmic level of IκBa and suppressed the nuclear level of p65 (Fig. 5E). These results suggested that SIRT6 may be an antineoplastic gene in PC by promoting ferroptosis and reducing glycolysis.

Discussion

PC is a highly malignant tumor of the digestive system and its 5-year survival rate is less than 8% (4). The specific pathogenesis of PC remains unclear. However, a large number of clinical and epidemiological studies have found that smoking, obesity, chronic pancreatitis and diabetes are important independent risk factors for PC (33). Previously, an increasing number of researchers have focused on the pathogenesis of PC, which may provide molecular targets for the diagnosis and treatment of PC (34). In the present study, it was found that the expression level of SIRT6 was lower in PC tissues and cells than in normal tissues and cells, and the low expression of SIRT6 was closely related to the poor prognosis (distant

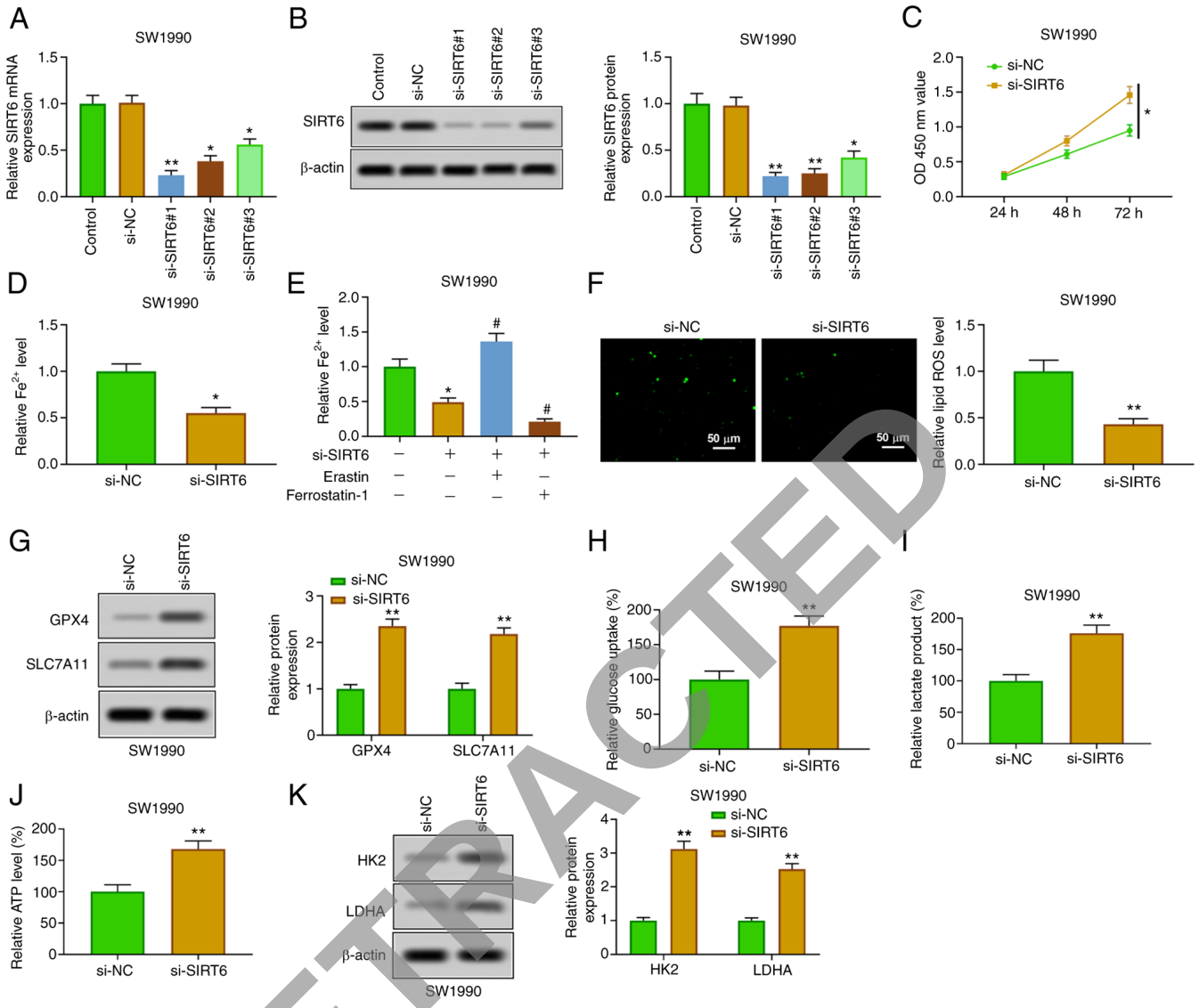

RETRACTED

Figure 3. Overexpression of SIRT6 induces ferroptosis and inhibits glycolysis in pancreatic cancer cells. (A and B) After transfection with si-SIRT6 (#1, #2 and #3), the expression of SIRT6 in PANC-1 cells was detected by reverse transcription-quantitative PCR and western blotting. (C) The viability of PANC-1 cells was determined by Cell Counting Kit-8 assay. (D) Fe^{2+} content was evaluated by Fe^{2+} detection kit. (E) PANC-1 cells transfected with si-SIRT6 were treated with erastin or ferrostatin-1, and then the Fe^{2+} content was evaluated by Fe^{2+} detection kit. (F) ROS level was detected by DCFH-DA method. (G) GPX4 and SLC7A11 expression levels were assessed by western blot analysis. (H-J) Glucose consumption, lactic acid and ATP production were evaluated by the corresponding kits. (K) HK2 and LDHA expression levels were detected by western blotting. *P<0.05 vs. control and si-NC group; **P<0.01 vs. control and si-NC group and $^{\#}$P<0.05 vs. SIRT6 group. SIRT6, sirtuin6; si-, small interfering; ROS, reactive oxygen species; GPX4, glutathione peroxidase 4; HK, hexokinase; LDHA, lactate dehydrogenase A.

metastasis, histological grade and TNM stages) of PC. In addition, the present results indicated that overexpression of SIRT6 improved PC *in vitro*, which was confirmed by the reduction of cell viability, the enhancement of ferroptosis and the inhibition of glycolysis. However, the silencing of SIRT6 enhanced the malignant degree of PC *in vitro*. In addition, SIRT6-mediated inhibition of NF-κB nuclear transcription may be related to its effect on ferroptosis and glycolysis in PC. The results of xenografted tumor experiment *in vivo* further verified that the upregulation of SIRT6 had obvious antitumor effect in PC.

PC has been demonstrated to rely on cysteine metabolism to prevent ferroptosis induced by ROS (35). SIRT6 could inhibit the growth of various malignant tumors (26,36,37). SIRT6 and SIRT6-mediated restraining of SIRT1 could induce head and neck cancers cell death by enhancing the level of intracellular ROS (38). SIRT6 also induced ROS-mediated glioma cell death (39). Furthermore, it has been reported that the overexpression of SIRT6 could resist cell viability and proliferation, block the cell cycle and accelerate apoptosis in gastric cancer through promoting the ferroptosis-inactivating JAK2/STAT3 signaling pathway (40). All these indicated that SIRT6 may play an anti-tumor role, and the present study confirmed this view in PC. The upregulation of SIRT6 could induce the increase of ROS and Fe^{2+} levels, inhibit the expression of GPX4 and SLC7A11 and induce ferroptosis in PC cells. However, the downregulation of SIRT6 showed the opposite effect. These finding indicated that SIRT6 played an anti-tumor role in PC by alleviating growth of tumor cells.

In addition, hypoxia and hypoxemia are important features of PC, which interact with glycolysis to promote the survival

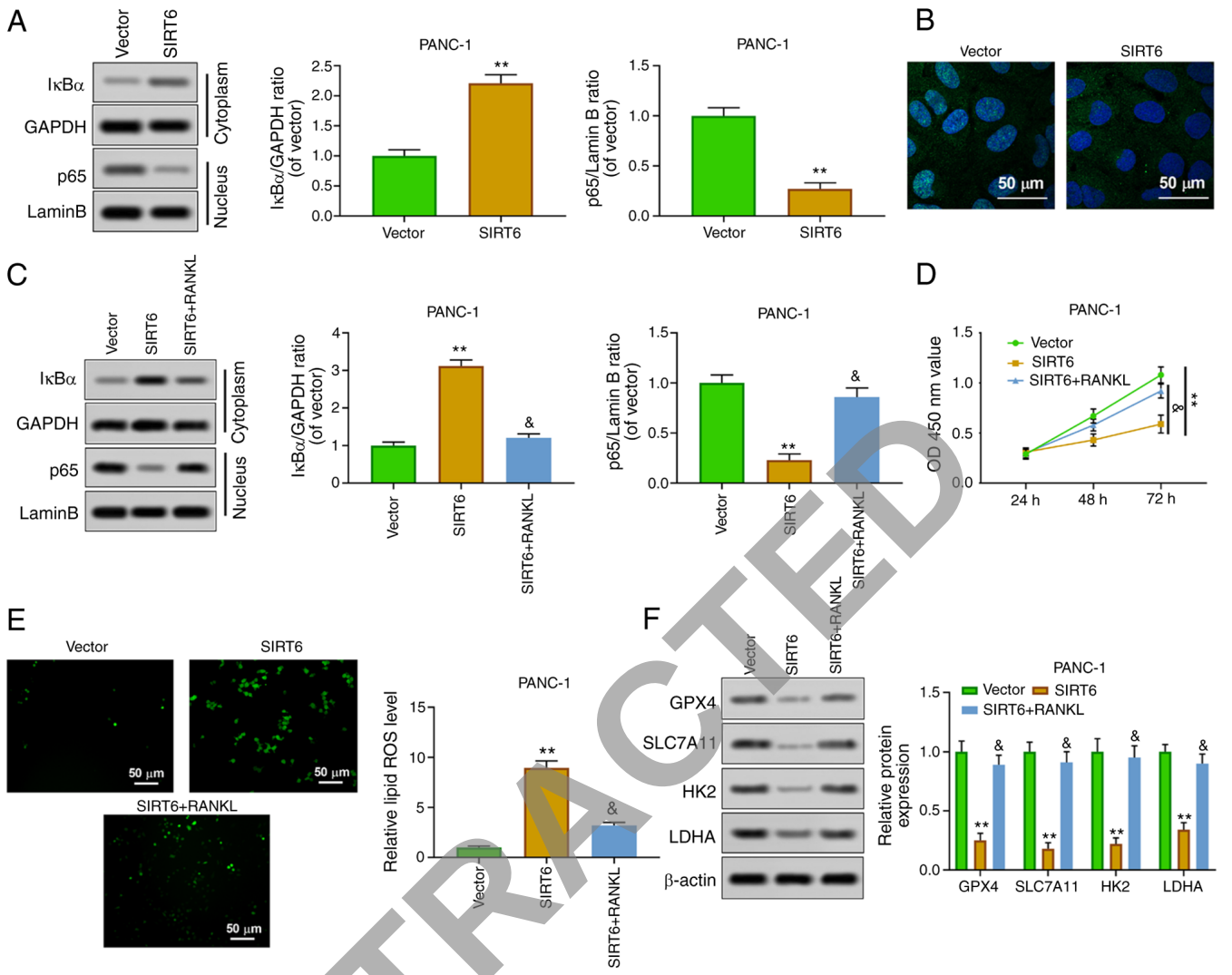

Figure 4. SIRT6 regulates the malignant phenotype of pancreatic cancer cells by activating the NF-κB pathway. (A) Nuclear NF-κB p65 and cytoplasmic IκBα protein levels were detected by western blot analysis. (B) Nuclear NF-κB p65 expression was evaluated by immunofluorescence. (C) PANC-1 cells were treated with vector, SIRT6, and SIRT6 + RANKL, and then nuclear NF-κB p65 and cytoplasmic IκBα protein levels were assessed by western blotting. (D) The viability of PANC-1 cells was evaluated by Cell Counting Kit-8 assay. (E) ROS level was detected by DCFH-DA method. (F) The expression levels of GPX4, SLC7A11, HK2 and LDHA were determined by western blotting. **P<0.01 vs. vector group and $^{\&}$P<0.05 vs. SIRT6 group. SIRT6, sirtuin6; ROS, reactive oxygen species; GPX4, glutathione peroxidase 4; HK, hexokinase; LDHA, lactate dehydrogenase A.

RETRACTED

and proliferation of tumor cells (19,41). Jiang *et al* (41) demonstrated that activated nuclear factor of activated T cells 5 (NFAT5) could promote glycolysis of PC cells by activating phosphoglycerate kinase 1, thereby further promoting a series of malignant biological behaviors such as tumor cell proliferation and invasion, and knockdown of NFAT5 has been proved to significantly improve this phenomenon *in vivo* and *in vitro*. SIRT6 was reported to be the regulator of glucose homeostasis (42). The inhibition of SIRT6 could promote the progression of lung cancer by enhancing glycolysis (43). SIRT6 could inhibit melanoma cell proliferation by inhibiting glycolysis (44). Similarly, the present study showed that the upregulation of SIRT6 reduced glucose uptake, lactose and ATP production, and inhibited the expression of HK2 and LDHA, which confirmed the inhibition of glycolysis. However, SIRT6 silencing promoted the occurrence of glycolysis. These results indicated that SIRT6 inhibited the growth of PC cells by promoting ferroptosis and inhibiting glycolysis.

It was reported that SIRT6 binds to the NF-κB subunit RELA and attenuates NF-κB signaling by modifying chromatin at NF-κB target genes (45). The transcription of NF-κB is involved in the regulation of ferroptosis and glycolysis (46,47). Aspirin induced the inhibition of NF-κB, which further weakened glycolysis in lung epithelial cells (48). TP53-induced glycolysis and apoptosis regulator, as the target gene of p53, could inhibit ROS and apoptosis in nasopharyngeal carcinoma by activating the NF-κB pathway (49). The inhibition of glycolysis mediated by tumor suppressor p53 is directly related to the inhibition of the IKK/NF-κB pathway (50). In the present study, the findings demonstrated that SIRT6 inhibited the nuclear transcription of NF-κB in PC cells. In order to confirm whether the SIRT6/NF-κB signaling pathway was involved in regulating the progression of PC, RANKL (NF-κB agonist) was used. The results revealed that RANKL could reverse the increase of ferroptosis and inhibition of glycolysis induced by SIRT6.

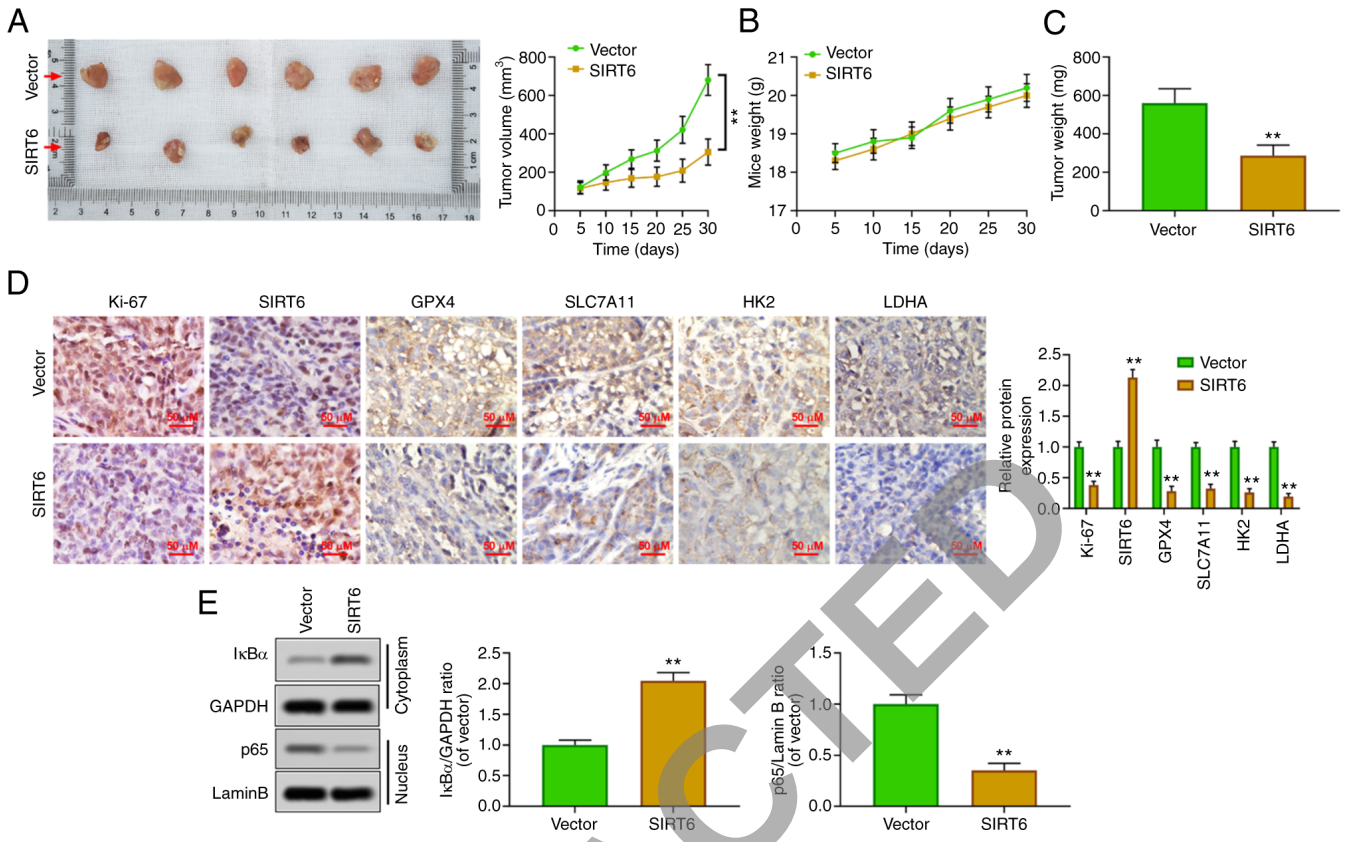

Figure 5. Upregulation of SIRT6 inhibits growth of pancreatic cancer xenografts *in vivo*. (A) Different groups of PANC-1 cells (vector and SIRT6-overexpressing) were inoculated subcutaneously (200 ml) in nude mice at a density of $1x10^6$/ml and the xenografted tumor size was measured every 7 days. After 28 days, the tumor was stripped from euthanized mice, and the tumor growth curve was drawn. (B and C) The body weight and xenografted tumor mass of nude mice were calculated. (D) The expression levels of GPX4, SLC7A11, HK2 and LDHA were assessed by immunohistochemistry. (E) Nuclear NF-κB p65 and cytoplasmic IkBα protein levels were detected by western blot analysis. $^{**}P<0.01$ vs. vector group. SIRT6, sirtuin6; GPX4, glutathione peroxidase 4; HK, hexokinase; LDHA, lactate dehydrogenase A.

RETRACTED

These results suggested that SIRT6 may affect PC through regulating the NF-κB signaling pathway.

In addition, *in vivo* experiments were performed to further confirm the antitumor activity of SIRT6. The data of the present study showed that the upregulation of SIRT6 inhibited the growth of xenografted tumors, attenuated the expression of ferroptosis-related protein and glycolysis-related protein and inhibited the nuclear transcription of NF-κB. These results further demonstrated that SIRT6 acted as an antitumor gene *in vivo*. However, there is a limitation to the present study; it was not investigated whether there is a necessary link between SIRT6-mediated ferroptosis and glycolysis, and further research will be carried out to explore this point.

In conclusion, the present study indicated that SIRT6 promoted ferroptosis and inhibited glycolysis in PC by regulating the NF-κB signaling pathway. SIRT6 may be a candidate target for the therapy of PC.

Acknowledgements

Not applicable.

Funding

The present study was supported by the Scientific research project of Hunan Provincial Health Commission (grant no. 202204012998) and the Hospital level scientific research fund project of The First Hospital of Changsha (grant no. Y2021-11).

Availability of data and materials

The datasets used and/or analyzed during the current study are available from the corresponding author on reasonable request.

Authors' contributions

JL conceived and designed the experiments. SG and LX performed the experiments and wrote the manuscript. ZL, QY, MH and YZ analyzed the data. JL made substantial contributions to proofreading the manuscript and gave final approval of the version to be published. JL and SG confirm the authenticity of all the raw data. All authors read and approved the final manuscript.

Ethics approval and consent to participate

Patient studies and animal experiments in the present study were approved [(2016) Ethical Review (Clinical Research) approval no. 59] by the Ethics Committee of The First Hospital of Changsha (Changsha, China). Written informed consent was provided by all participants.

Patient consent for publication

Not applicable.

Competing interests

The authors declare that they have no competing interests.

References

1. Neoptolemos JP, Kleeff J, Michl P, Costello E, Greenhalf W and Palmer DH: Therapeutic developments in pancreatic cancer: Current and future perspectives. Nat Rev Gastroenterol Hepatol 15: 333-348, 2018.
2. Zhang L, Sanagapalli S and Stoita A: Challenges in diagnosis of pancreatic cancer. World J Gastroenterol 24: 2047-2060, 2018.
3. Zeng S, Pöttler M, Lan B, Grützmann R, Pilarsky C and Yang H: Chemoresistance in pancreatic cancer. Int J Mol Sci 20: 4504, 2019.
4. Gupta R, Amanam I and Chung V: Current and future therapies for advanced pancreatic cancer. J Surg Oncol 116: 25-34, 2017.
5. Collisson EA, Bailey P, Chang DK and Biankin AV: Molecular subtypes of pancreatic cancer. Nat Rev Gastroenterol Hepatol 16: 207-220, 2019.
6. Jentzsch V, Davis JAA and Djamgoz MBA: Pancreatic Cancer (PDAC): Introduction of evidence-based complementary measures into integrative clinical management. Cancers (Basel) 12: 3096, 2020.
7. Jonckheere N, Vasseur R and Van Seuningen I: The cornerstone K-RAS mutation in pancreatic adenocarcinoma: From cell signaling network, target genes, biological processes to therapeutic targeting. Crit Rev Oncol Hematol 111: 7-19, 2017.
8. Hirschhorn T and Stockwell BR: The development of the concept of ferroptosis. Free Radic Biol Med 133: 130-143, 2019.
9. Mou Y, Wang J, Wu J, He D, Zhang C, Duan C and Li B: Ferroptosis, a new form of cell death: Opportunities and challenges in cancer. J Hematol Oncol 12: 34, 2019.
10. Ye Z, Zhuo Q, Hu Q, Xu X, Mengqi Liu, Zhang Z, Xu W, Liu W, Fan G, Qin Y, *et al*: FBW7-NRA41-SCD1 axis synchronously regulates apoptosis and ferroptosis in pancreatic cancer cells. Redox Biol 38: 101807, 2021.
11. Yang WH, Ding CC, Sun T, Rupprecht G, Lin CC, Hsu D and Chi JT: The hippo pathway effector TAZ regulates ferroptosis in renal cell carcinoma. Cell Rep 28: 2501-2508.e4, 2019.
12. Sun X, Ou Z, Chen R, Niu X, Chen D, Kang R and Tang D: Activation of the p62-Keap1-NRF2 pathway protects against ferroptosis in hepatocellular carcinoma cells. Hepatology 63: 173-184, 2016.
13. Jinesh GG, Sambandam V, Vijayaraghavan S, Balaji K and Mukherjee S: Molecular genetics and cellular events of K-Ras-driven tumorigenesis. Oncogene 37: 839-846, 2018.
14. Rabi T and Catapano CV: Aphanin, a triterpenoid from Amoora rohituka inhibits K-Ras mutant activity and STAT3 in pancreatic carcinoma cells. Tumour Biol 37: 12455-12464, 2016.
15. Xia X, Fan X, Zhao M and Zhu P: The relationship between ferroptosis and tumors: A novel landscape for therapeutic approach. Curr Gene Ther 19: 117-124, 2019.
16. Zhu S, Zhang Q, Sun X, Zeh HJ III, Lotze MT, Kang R and Tang D: HSPA5 regulates ferroptotic cell death in cancer cells. Cancer Res 77: 2064-2077, 2017.
17. Yang J, Xu J, Zhang B, Tan Z, Meng Q, Hua J, Liu J, Wang W, Shi S, Yu X and Liang C: Ferroptosis: At the crossroad of gemcitabine resistance and tumorigenesis in pancreatic cancer. Int J Mol Sci 22: 10944, 2021.
18. Xu G, Wang H, Li X, Huang R and Luo L: Recent progress on targeting ferroptosis for cancer therapy. Biochem Pharmacol 190: 114584, 2021.
19. Yang J, Ren B, Yang G, Wang H, Chen G, You L, Zhang T and Zhao Y: The enhancement of glycolysis regulates pancreatic cancer metastasis. Cell Mol Life Sci 77: 305-321, 2020.
20. Jiao L, Zhang HL, Li DD, Yang KL, Tang J, Li X, Ji J, Yu Y, Wu RY, Ravichandran S, *et al*: Regulation of glycolytic metabolism by autophagy in liver cancer involves selective autophagic degradation of HK2 (hexokinase 2). Autophagy 14: 671-684, 2018.
21. DeWaal D, Nogueira V, Terry AR, Patra KC, Jeon SM, Guzman G, Au J, Long CP, Antoniewicz MR and Hay N: Hexokinase-2 depletion inhibits glycolysis and induces oxidative phosphorylation in hepatocellular carcinoma and sensitizes to metformin. Nat Commun 9: 446, 2018.
22. Yang J, Ma S, Xu R, Wei Y, Zhang J, Zuo T, Wang Z, Deng H, Yang N and Shen Q: Smart biomimetic metal organic frameworks based on ROS-ferroptosis-glycolysis regulation for enhanced tumor chemo-immunotherapy. J Control Release 334: 21-33, 2021.
23. Singh CK, Chhabra G, Ndiaye MA, Garcia-Peterson LM, Mack NJ and Ahmad N: The role of Sirtuins in antioxidant and redox signaling. Antioxid Redox Signal 28: 643-661, 2018.
24. Liu L, Li Y, Cao D, Qiu S, Li Y, Jiang C, Bian R, Yang Y, Li L, Li X, *et al*: SIRT3 inhibits gallbladder cancer by induction of AKT-dependent ferroptosis and blockade of epithelial-mesenchymal transition. Cancer Lett 510: 93-104, 2021.
25. Lee J, You JH, Kim MS and Roh JL: Epigenetic reprogramming of epithelial-mesenchymal transition promotes ferroptosis of head and neck cancer. Redox Biol 37: 101697, 2020.
26. Sebastián C, Zwaans BM, Silberman DM, Gymrek M, Goren A, Zhong L, Ram O, Truelove J, Guimaraes AR, Toiber D, *et al*: The histone deacetylase SIRT6 is a tumor suppressor that controls cancer metabolism. Cell 151: 1185-1199, 2012.
27. Tasselli L, Zheng W and Chua KF: SIRT6: Novel mechanisms and links to aging and disease. Trends Endocrinol Metab 28: 168-185, 2017.
28. Liu G, Chen H, Liu H, Zhang W and Zhou J: Emerging roles of SIRT6 in human diseases and its modulators. Med Res Rev 41: 1089-1137, 2021.
29. Kugel S, Sebastián C, Fitamant J, Ross KN, Saha SK, Jain E, Gladden A, Arora KS, Kato Y, Rivera MN, *et al*: SIRT6 suppresses pancreatic cancer through control of Lin28b. Cell 165: 1401-1415, 2016.
30. Zwaans BM and Lombard DB: Interplay between sirtuins, MYC and hypoxia-inducible factor in cancer-associated metabolic reprogramming. Dis Models Mech 7: 1023-1032, 2014.
31. Zhang C, Yu Y, Huang Q and Tang K: SIRT6 regulates the proliferation and apoptosis of hepatocellular carcinoma via the ERK1/2 signaling pathway. Mol Med Rep 20: 1575-1582, 2019.
32. Livak KJ and Schmittgen TD: Analysis of relative gene expression data using real-time quantitative PCR and the 2(-Delta Delta C(T)) method. Methods 25: 402-408, 2001.
33. Goral V: Pancreatic cancer: Pathogenesis and diagnosis. Asian Pac J Cancer Prev 16: 5619-5624, 2015.
34. Grant TJ, Hua K and Singh A: Molecular pathogenesis of pancreatic cancer. Prog Mol Biol Transl Sci 144: 241-275, 2016.
35. Badgley MA, Kremer DM, Maurer HC, DelGiorno KE, Lee HJ, Purohit V, Sagalovskiy IR, Ma A, Kapilian J, Firl CEM, *et al*: Cysteine depletion induces pancreatic tumor ferroptosis in mice. Science 368: 85-89, 2020.
36. Cai M, Hu Z, Han L and Guo R: MicroRNA-572/hMOF/Sirt6 regulates the progression of ovarian cancer. Cell Cycle 19: 2509-2518, 2020.
37. Liu W, Wu M, Du H, Shi X, Zhang T and Li J: SIRT6 inhibits colorectal cancer stem cell proliferation by targeting CDC25A. Oncol Lett 15: 5368-5374, 2018.
38. Park JJ, Hah YS, Ryu S, Cheon SY, Won SJ, Lee JS, Hwa JS, Seo JH, Chang HW, Kim SW and Kim SY: MDM2-dependent Sirt1 degradation is a prerequisite for Sirt6-mediated cell death in head and neck cancers. Exp Mol Med 53: 422-431, 2021.
39. Chen X, Li D, Gao Y, Cao Y and Hao B: Histone deacetylase SIRT6 inhibits glioma cell growth through down-regulating NOTCH3 expression. Acta Biochim Biophys Sin (Shanghai) 50: 417-424, 2018.
40. Cai S, Fu S, Zhang W, Yuan X, Cheng Y and Fang J: SIRT6 silencing overcomes resistance to sorafenib by promoting ferroptosis in gastric cancer. Biochem Biophys Res Commun 577: 158-164, 2021.
41. Jiang Y, He R, Jiang Y, Liu D, Tao L, Yang M, Lin C, Shen Y, Fu X, Yang J, *et al*: Transcription factor NFAT5 contributes to the glycolytic phenotype rewiring and pancreatic cancer progression via transcription of PGK1. Cell Death Dis 10: 948, 2019.
42. Zhong L, D'Urso A, Toiber D, Sebastian C, Henry RE, Vadysirisack DD, Guimaraes A, Marinelli B, Wikstrom JD, Nir T, *et al*: The histone deacetylase Sirt6 regulates glucose homeostasis via Hif1alpha. Cell 140: 280-293, 2010.
43. Fang C, Liu Y, Chen L, Luo Y, Cui Y, Zhang N, Liu P, Zhou M and Xie Y: α-Hederin inhibits the growth of lung cancer A549 cells in vitro and in vivo by decreasing SIRT6 dependent glycolysis. Pharm Biol 59: 11-20, 2021.

RETRACTED

44. Dong Z, Yang J, Li L, Tan L, Shi P, Zhang J, Zhong X, Ge L, Wu Z and Cui H: FOXO3a-SIRT6 axis suppresses aerobic glycolysis in melanoma. Int J Oncol 56: 728-742, 2020.
45. Santos-Barriopedro I, Bosch-Presegué L, Marazuela-Duque A, de la Torre C, Colomer C, Vazquez BN, Fuhrmann T, Martínez-Pastor B, Lu W, Braun T, *et al*: SIRT6-dependent cysteine monoubiquitination in the PRE-SET domain of Suv39h1 regulates the NF-κB pathway. Nat Commun 9: 101, 2018.
46. Moretti M, Bennett J, Tornatore L, Thotakura AK and Franzoso G: Cancer: NF-κB regulates energy metabolism. Int J Biochem Cell Biol 44: 2238-2243, 2012.
47. Gao J, Luo T and Wang J: Gene interfered-ferroptosis therapy for cancers. Nat Commun 12: 5311, 2021.
48. Cuesta E, Boada J, Perales JC, Roig T and Bermudez J: Aspirin inhibits NF-kappaB activation in a glycolysis-depleted lung epithelial cell line. Eur J Pharmacol 517: 158-164, 2005.
49. Zhao M, Fan J, Liu Y, Yu Y, Xu J, Wen Q, Zhang J, Fu S, Wang B, Xiang L, *et al*: Oncogenic role of the TP53-induced glycolysis and apoptosis regulator in nasopharyngeal carcinoma through NF-κB pathway modulation. Int J Oncol 48: 756-764, 2016.
50. Kawauchi K, Araki K, Tobiume K and Tanaka N: p53 regulates glucose metabolism through an IKK-NF-κB pathway and inhibits cell transformation. Nat Cell Biol 10: 611-618, 2008.

This work is licensed under a Creative Commons Attribution-NonCommercial-NoDerivatives 4.0 International (CC BY-NC-ND 4.0) License.

RETRACTED